Natural visual behavior in individuals with peripheral visual-field loss

Ricardo Ramos Gameiro Institute of Cognitive Science, University of Osnabrück, Osnabrück, Germany

Kristin Jünemann Institute of Cognitive Science, University of Osnabrück, Osnabrück, Germany

Anne Herbik Visual Processing Lab, Ophthalmic Department, Otto-von-Guericke-University Magdeburg, Magdeburg, Germany

Anika Wolff Visual Processing Lab, Ophthalmic Department, Otto-von-Guericke-University Magdeburg, Magdeburg, Germany

Peter König* Institute of Cognitive Science, University of Osnabrück, Osnabrück, Germany; Institute of Neurophysiology und Pathophysiology, University Medical Center Hamburg-Eppendorf, Hamburg, Germany

Michael B. Hoffmann* Visual Processing Lab, Ophthalmic Department, Otto-von-Guericke-University Magdeburg, Magdeburg, Germany; Center for Behavioral Brain Sciences, Magdeburg, Germany

Retinitis pigmentosa (RP) is an inherited disease that causes progressive peripheral visual-field loss. In this study, we investigated how such loss affects visual exploration of natural images. Individuals with varying degrees of visual-field loss and healthy control participants freely observed images of different sizes while eye movements were recorded. We examined whether visual behavior differed when the scene content was shown in various extents of the visual field, and investigated the spatial bias, saccade amplitudes, and number and duration of fixations. We found that the healthy control group showed a central spatial bias during image viewing. The RP group showed similar biases on the group level, but with reproducible individual exploration patterns. For saccade amplitudes, the healthy control group and the RP group showed similar behavior throughout all image sizes. The RP group with severe loss of peripheral vision thus tended to target saccades toward blind areas of their visual field. The number of fixations did not change between the two groups, although fixation durations decreased in the RP group. In conclusion, the RP group scanned the images surprisingly similarly to the healthy control group; however, they showed individual idiosyncratic explorative strategies when the observed scene exceeded their visible field. Thus, although RP leads to a severe loss of the visual field, there is no general adaptive mechanism to change visual exploration. Instead, individuals rely on individual strategies, leading to high heterogeneity in the RP group.

Introduction

The human visual field spans a large area and provides rich information (Loschky, Fortenbaugh, &

Citation: Ramos Gameiro, R., Jünemann, K., Herbik, A., Wolff, A., König, P., Hoffmann, M. B. (2018). Natural visual behavior in individuals with peripheral visual-field loss. *Journal of Vision*, *18*(12):10, 1–21, https://doi.org/10.1167/18.12.10.

https://doi.org/10.1167/18.12.10 Received April 13, 2018; published November 20, 2018 ISSN 1534-7362

Levi, 2017). However, as the brain provides only limited capacity to process visually available information simultaneously (Broadbent, 1958; Desimone & Duncan, 1995; Egeth, 1967; Wahn & König, 2015), we have to selectively focus on a small part of our environment (Geisler & Cormack, 2011; Liversedge & Findlay, 2000; Posner, 1980). Thus, when the gaze is directed toward a region of interest, the majority of in-depth visual information gained refers to only a small fraction of the visual field (Rosenholtz, Huang, Raj, Balas, & Ilie, 2012). This focused spotlight of information processing is described as *overt attention* and lies in the foveal part of the eyes (Kaspar, 2013; Loschky et al., 2017; Posner, 1980; Rosenholtz et al., 2012). Consequently, overt attention as described by eye fixations provides detailed insights into information processing in visual perception. Compared to foveal processing, information processing in the peripheral area of the retina outside of the foveal spotlight is less reliable (Rosenholtz et al., 2012; Rosenholtz, 2016; Staugaard, Petersen, & Vangkilde, 2016), but still of great importance, for example during object identification outside of the fovea (Boucart et al., 2016; Boucart, Moroni, Thibaut, Szaffarczyk, & Greene, 2013; Henderson & Anes, 1994). This peripheral information processing is described as *covert attention* (Carrasco, 2011; Kaspar & König, 2012; Posner, 1980). To enhance the crude peripheral information processing (Rosenholtz et al., 2012), the covertly attended peripheral region is overtly attended by initiation of a saccade (Loschky et al., 2017; Posner, 1980; Rosenholtz et al., 2012)—that is, a fixation shift into the covertly attended peripheral region (Deubel & Schneider, 1996; Fischer & Breitmeyer, 1987; Hoffman & Subramaniam, 1995). In natural free image viewing, fixation and planning the next saccade therefore provides an update to decide where to look next, several times per second (Kowler, 2011). Thus, the interplay between overt and covert attention—that is, central and peripheral vision—is crucial for the dynamics of visual behavior in order to maintain a fluent and constant visual exploration of the environment.

Individuals with advanced retinitis pigmentosa (RP) experience a loss of peripheral vision (Hartong, Berson, & Dryja, 2006) due to the gradual degeneration of photoreceptors in the retina beginning in the periphery and slowly progressing to the central part of the retina (Berson, Sandberg, Rosner, Birch, & Hanson, 1985; Hamel, 2006; Parmeggiani et al., 2011). As peripheral cues in the visual field normally guide visual attention and thus provide where to look next during image observation (Deubel & Schneider, 1996; Fischer & Breitmeyer, 1987; Hoffman & Subramaniam, 1995; Najemnik & Geisler, 2005; Rajashekar, Bovik, & Cormack, 2006), saccade planning based on peripheral cues should be impaired in advanced RP by the decreased interplay between overt and covert attention. Due to the gradual nature of the visual decline in RP (Berson et al., 1985; Hamel, 2006), adaptations of the visual system might lead to alterations of visual exploration. However, due to stable motor constraints in the saccadic system leading to a preference for making smaller rather than larger saccades (Bahill, Adler, & Stark, 1975; Gajewski, Pearson, Mack, Bartlett, & Henderson, 2004; Pelz & Canosa, 2001; Tatler, Baddeley, & Vincent, 2006), adaptive visual behavior is not expected to affect saccade amplitudes. Indeed, we have previously shown in healthy observers that the log-normal baseline distribution of saccade amplitudes even remains stable independent of the perceived amount of image content (Ramos Gameiro, Kaspar, König, Nordholt, & König, 2017). This hypothesis is supported by Luo, Vargas-Martin, and Peli (2008), who have shown that individuals with tunnel vision did not adapt saccade amplitudes in free viewing. Due to these stable saccade amplitudes, individuals with RP might adapt exploration in terms of the number of fixations in free viewing. As a consequence, visual information processing (i.e., conscious extraction of meaning and relevance from the fixated region) would be reduced (Ramos Gameiro et al., 2017), showing that individuals with RP do not process the fixated region in full depth (Unema, Pannasch, Joos, & Velichkovsky, 2005). In conclusion, individuals with RP might develop individual characteristics in natural visual behavior to compensate for the lack of peripheral vision and covert attention. In the present study, we investigated to what extent a loss of peripheral vision in individuals with RP with varying degrees of disease progression affects natural visual behavior.

Rationale and hypotheses

Here we explore visual exploration and its properties in individuals with RP in a free-viewing paradigm. A healthy control group and an RP group were confronted with natural static images while their eye movements were recorded. We varied the presented size of the images, at 7, 15, and 30 in., to compare the explorative behavior for stimuli covering the residual as well as the defective visual field or only the residual visual field in the RP group. We then examined the spatial bias by measuring the central tendency as well as the entropy (Bindemann, 2010; Parkhurst & Niebur, 2003; Ramos Gameiro et al., 2017; Tatler, 2007). Saccade amplitudes provided a further estimate of the visual exploration, by describing the distance between two consecutive fixations. The number of fixations made by an observer was taken as a measure for visual exploration. For measuring the in-depth information-

processing time of the fixated image region, we use the measure of fixation duration (Unema et al., 2005).

We stated three major hypotheses on visual exploratory behavior in individuals with RP. They highlight complementary potential effects on the tested oculomotor parameters:

Hypothesis 1

Individuals with RP will compensate for the missing peripheral cues by an increased active visual-search strategy to gain full semantic knowledge of the image scenery. Compared to the healthy control group, this leads to a reduced central tendency with a scattered structure of fixations. This will be captured by a weaker spatial bias and increased entropy. Further, this active image scanning will be more pronounced in individuals with more severe visual-field loss and in large image sizes. Specifically, individuals with a severe progress of RP will target many saccades toward blind peripheral regions to compensate for the missing peripheral cues.

Hypothesis 2

Due to stable motor constraints in the saccadic system that are not affected by the disease, we the distribution of saccade amplitudes will remain constant in individuals with RP (Gajewski et al., 2004; Pelz & Canosa, 2001; Tatler et al., 2006). As a consequence, those with severe progress of the disease will target many saccades outside of their visual field.

Hypothesis 3

Given a weaker central tendency and stable oculomotor constraints in the saccadic system (Martinez-Conde, Macknik, & Hubel, 2004), individuals with RP will make strategic adjustments to their visual exploratory behavior. This will be captured by an increased number of fixations with reduced single fixation durations. As a consequence, the RP group will sacrifice depth of visual information processing (Cohen, McClure, & Yu, 2007; Ramos Gameiro et al., 2017), as indicated by shorter fixation durations (Unema et al., 2005).

Methods

This study was conducted in the Neurobiopsychology Laboratory at the Institute of Cognitive Science of the University of Osnabrück, Germany (eye-movement recordings of control group) and in the visual-processing laboratory of the ophthalmic department at the Otto-von-Guericke-University in Magdeburg, Germany (eye-movement recordings of the RP group). The experimental methods were approved by the ethical committees of the University of Osnabrück and the University of Magdeburg, Germany, and performed in accordance with the guidelines of the German Psychological Society. This experiment conformed to the Declaration of Helsinki. All participants gave written informed consent to participate before the examination.

Participants

Twenty healthy participants (17 females, three male; ages 17–28 years, $M = 20$, $SD = 2.42$) with normal or corrected-to-normal vision took part in this study. These healthy participants were labeled the control group. Seventeen participants with RP (eight female, nine male; ages 25–67 years, $M = 51$, $SD = 12.75$) took part in this study. The individuals with RP varied in their progress of visual-field loss and thus peripheral vision (visual-field size approximately 1.8°–18.5°, as detailed later). All participants (both groups) were instructed to freely observe the stimuli on the screen.

Perimetry test

Mean defect

We used standardized perimetry to determine visual-field defects in the RP group within the central ±30°. Specifically, light-spot detection thresholds were determined with automated static white-on-white perimetry (Octopus 101 Perimeter, Haag-Streit, Köniz, Switzerland) using the program dG2, comprising 59 test positions as depicted in Figure 1a (background luminance = 1.27 cd/m^2; target size = Goldmann size III [0.4° diameter]; target exposition = 100 ms; Weber & Klimaschka, 1995). The RP group fixated centrally on a cross with a central gap (to allow testing of the foveal sensitivity) while target dots appeared randomly in the visual field. Target detection was reported via button press.

Visual-field size

To obtain a measure of the RP participants' residual central visual fields, we calculated the visual-field size in visual degrees based on the location for which an absolute scotoma (black squares in Figure 1a) was absent. Specifically, in relation to the total circular size of the template (60° visual angle), we computed the radius of the circle with the same area as the residual visual field of the patient (Figure 1b). Consequently, a larger number of seen target dots implied a larger radius. Figure 1c shows a cumulative distribution

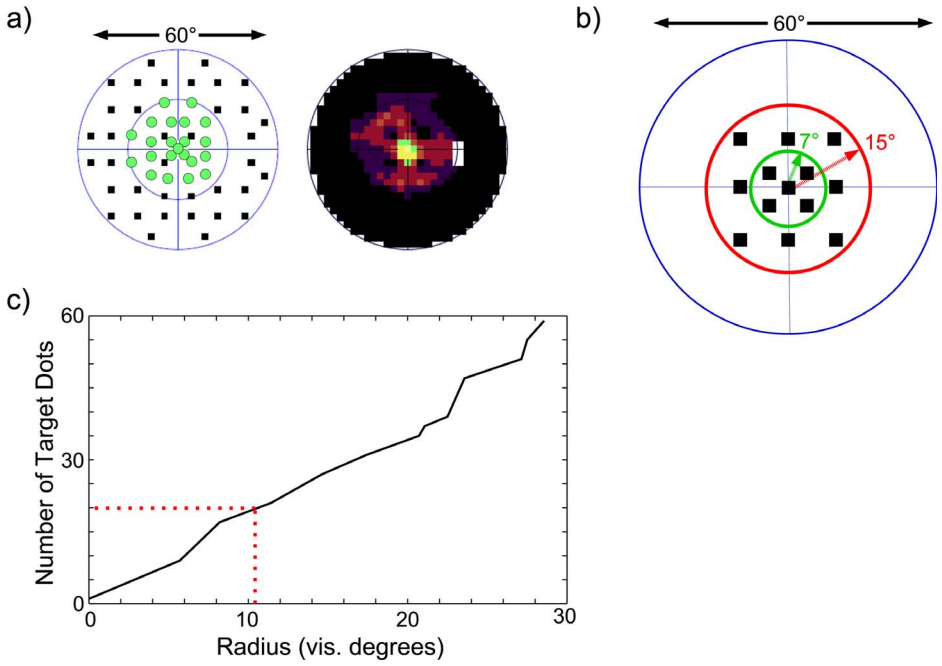

Figure 1. (a) Left side: Perimetry results for the right eye of an example individual with retinitis pigmentosa with relative and absolute visual-field defects (green and black dots, respectively). Right side: Visualization of the visual field of the same patient. Lighter colors indicate higher retinal sensitivity. The white rectangle represents the blind spot, which is spared from the perimetric measurements. (b) Sketch showing how we calculated the visual-field size in degrees of visual angle. The black dots were combined in circles from center to periphery. The size of the circles was examined in relation to the total size of the perimetry chart (diameter 60°). Here as an example: Central vision of five dots represents a visual-field size of 7° (green circle), and 13 dots represent 15° (red circle). (c) Estimation of the visual-field size of the example individual in (a), based on the cumulative distribution function: 21 visible dots represent a visual-field size of ~11.9°.

indicating the radius of the circle based on the number of target dots that fall into the respective area. With respect to the cumulative distribution function, the related radius of this number of target dots described the visual-field size of the observer (Figure 1c).

Apparatus

The stimuli were presented on a 30-in. (46.5° × 29.1°) widescreen Apple Cinema HD display with a native resolution of 2,560 × 1,600 pixels. For eye-movement recordings, we used a remote EyeLink 1000 eye tracker (SR Research Ltd., Ottawa, Canada) providing monocular recordings with one eye camera and a sample rate of 500 Hz. By default of the EyeLink system, saccade detection was based on velocity (>30°/s) and acceleration (>8,000°/s^2). One or both of these criteria had to be met in order to trigger a saccade. This trigger had to be maintained for at least 4 ms to detect a saccade. The onset of the saccade was defined as when the spatial location of the eye position exceeded a motion threshold of at least 0.1°. Periods without saccade detection were labeled as fixations.

We positioned the eye tracker on a table between the participant and the monitor, such that the stimuli on the monitor were completely observable and not partially covered by the eye tracker. Participants were seated in a darkened room at a distance of 70 cm from the monitor, resulting in 51.7 pixels/visual degree in the center of the monitor. We did not still the participants' heads with a headrest, to facilitate comfortable conditions, but we verbally instructed participants not to make head movements during the experiment. The experimenter constantly observed the participants to make sure that their heads remained stable during the recordings. Although we instructed them to remain still, we used the head-tracking feature of the EyeLink system to guarantee stable gaze recordings based on eye movements independent of residual involuntary head movements. Hence, head movements of the participants during the experiment were close to none. In cases of small involuntary manifestations of head movements, the EyeLink system corrected eye position accordingly.

Before the actual recordings, we determined the dominant eye of each participant using the Rosenbach (1903) sighting test. The dominant eye was then used for experimental recordings. Note that the monocular eye selection was done only for the eye recordings; participants still viewed the stimuli binocularly. In order to calibrate the eye-tracking camera, we followed

standard procedures (Ramos Gameiro et al., 2017; Wilming et al., 2017). Briefly, each participant had to fixate on nine black circles (~0.5°) that appeared consecutively at different screen locations. The calibration was validated afterward by calculating the drift error for each point. As some RP participants had a very narrow visual field and could not find peripheral fixation dots themselves, we verbally guided these participants' gazes to the location of the black circles (e.g., "the current calibration dot is in the upper left corner"). The calibration was repeated until the system reached an average accuracy of <0.5° for the control group and <1.0° for the RP group (due to impaired vision).

The experiment took place in two different locations with the same equipment. We initially recorded the control group at the University of Osnabrück, Germany, and then transported all necessary computers, the monitor, the remote eye tracker, and additional complements to the University of Magdeburg, Germany. Thus, the experimental setup and arrangement of hardware were identical in both laboratories. Both laboratories were of similar size. We darkened the laboratories during eye-movement recordings, such that objects in the laboratory would not distract the participants.

Stimuli

We used 240 static photographs containing natural environments (e.g., landscapes, urban scenes). All photographs were obtained from the internal image database of the Neurobiopsychology Laboratory at the University of Osnabrück, Germany, and have already been used in previous studies (Ramos Gameiro et al., 2017; Wilming et al., 2017). By bicubic interpolation, we scaled each image up to 2,560 × 1,600 pixels to match the full-size screen resolution of the display monitor (30 in. diagonal; 46.5° × 29.1°). Based on this full-size screen resolution, we gradually reduced the image size during the experiment by two more levels, according to the following equations:

$$y_d = \frac{1}{2 \times L} \times 1,600 \quad (1)$$

and

$$x_d = \frac{1}{2 \times L} \times 2,560, \quad (2)$$

where y_d and x_d denote the desired x- and y-resolution of the image size, and L denotes the level of image-size reduction (here, $L = 1$ or 2). This gradual image-size reduction resulted in scaled image sizes of 1,280 × 800 pixels (~15 in. diagonal; 23.3° × 14.5°) and 640 × 400 pixels (~7 in. diagonal; 11.6° × 7.3°).

Figure 2. (a) Example image used in this experiment in 30-in. full-screen size as well as downsized to 15 and 7 in. according to the scaled (upper row) and cropped (lower row) condition. (b) Sample procedure of one of four sessions including three randomized blocks. Across blocks, the image size was distinct. Within each block, 10 scaled and 10 cropped images of the same size were randomly presented.

Furthermore, we manipulated the images in two ways. Following our previous study (Ramos Gameiro et al., 2017), we either scaled the images, leading to a presentation of the whole image scenery but at a smaller size, or cropped out the central part of the image, thus presenting only this central part but at the same resolution as in the large image. For the cropped condition, we extracted the corresponding central section of the full-size image (Figure 2a). With this method we could compare whether differences in visual behavior indeed relied on changes of spatial properties of the image (image size) or solely on varying spatial properties of regions of interest within the images (size of objects). The background color of reduced-size images was set to neutral gray (RGB: 128/128/128).

Procedure

The experiment was divided into four equally long sessions. Each session consisted of 60 images and followed a calibration of the eye-tracking system. Within each session, we presented three blocks of 20 equally sized images. Half of the images were scaled and the other half cropped. In blocks containing 30-in. images, we randomly labeled half of the images as cropped for statistical purposes. The blocks within each

	7-in. scaled	15-in. scaled	30-in. scaled	7-in. cropped	15-in. cropped	30-in. cropped
RP group	9.71%	6.25%	4.98%	8.66%	5.33%	5.20%
Control group	7.15%	4.81%	3.50%	6.91%	4.47%	3.26%
t	2.012	1.357	1.968	1.332	0.770	2.719
p	0.052	0.183	0.057	0.191	0.446	0.010

Table 1. Percentage of excluded fixations for the retinitis pigmentosa (RP) and control groups, averaged over participants and trials. The lower two rows show the results (*t*-test *t* and *p* values; Bonferroni-adjusted $\alpha = 0.008$) of the individual contrasts between RP- and control-group participants regarding the number of excluded fixations.

session were also randomized in order (Figure 2b). The images were centered on the display monitor and presented for 6 s each (Ramos Gameiro et al., 2017). Each participant saw each image only once during the experiment. Before each image presentation (trial), the participants had to fixate a central fixation dot that was additionally used for drift correction.

Dependent variables

We used different standard eye-tracking parameters for statistical analysis of the data. These parameters included the number and mean duration of fixations, as well as saccade amplitudes. We further analyzed the spatial distribution of fixations and their respective entropy.

Number and mean duration of fixations

For the number of fixations, we added up all fixations within each trial. The first fixation of each trial was excluded, as it was a direct consequence of the central drift correction preceding the trial. All fixations located outside of the corresponding image coordinates were also excluded (see Table 1). As Table 1 shows, the amount of excluded data did not largely differ between the RP and control groups (all ts ≤ 2.719; all ps ≥ 0.010, with Bonferroni-adjusted alpha level $\alpha = 0.008$). Hence, we expected no relevant effects of our exclusion criteria for the analyses comparing both groups.

For measuring the in-depth information-processing time of the fixated image region, we employed the measure of fixation durations (Unema et al., 2005). For the mean duration of fixations, we subtracted the temporal onset from the temporal offset. These times were automatically determined by the eye tracker during the experiment. To avoid biased results from outliers, we excluded fixation durations of less than 50 ms and of two standard deviations above the grand mean (RP group: cutoff at 620.77 ms; control group: cutoff at 798.40 ms) over all participants (Ramos Gameiro et al., 2017). In all ongoing analyses, we used only fixations that did not meet our exclusion criteria. These fixations were labeled as *valid fixations*.

Saccade amplitudes

Saccades were taken as a measure for visual exploration. We characterized saccade amplitudes by calculating the Euclidean distance between the two-dimensional coordinates of two sequential fixations. We excluded saccade amplitudes in our analysis if either the corresponding pre- or postfixation of the saccade was located outside of the image coordinates (Table 2). The exclusion of saccade amplitudes did not significantly differ in all tested image sizes (all ts ≤ 2.608; all ps ≥ 0.013, with Bonferroni-adjusted alpha level $\alpha = 0.008$), except for cropped 30-in. images ($t = 2.810$; $p = 0.008$, with Bonferroni-adjusted alpha level $\alpha = 0.008$). This exclusion of data was done to prevent adding saccade amplitudes into the analyses that were longer than the presented images themselves. Consequently, in this study we analyzed the amplitudes of saccades made only within images, for increased transparency and reproducibility of the experimental design.

Note that although the RP group had reduced visual information of the image borders, we excluded fixations outside of these borders in order to have a well-controlled paradigm that follows standard practices to exclude all data where experimental instructions were violated (i.e., visually explore the images). In our experimental design, we presented same-size images sequentially in blocks. Hence, RP participants were able to constantly obtain a general knowledge of each image size.

Regarding saccades, each off-fixation outside the image coordinates was involved in two saccades—the one leading to that fixation and the one originating at that location. To guarantee experimental validity, we took a conservative approach and excluded both types of saccades. This results in constraints regarding a natural setting—that is, the experimental investigation is limited to the finite size of the stimulus—but it is well controlled and reproducible in future experiments.

Spatial fixation bias and entropy

The spatial bias was examined by the central tendency as well as entropy. The central tendency captured the spatial bias as a measure toward central image regions (Bindemann, 2010; Parkhurst & Niebur,

	7-in. scaled	15-in. scaled	30-in. scaled	7-in. cropped	15-in. cropped	30-in. cropped
RP group	31.92%	25.37%	22.89%	32.38%	24.68%	23.23%
Control group	27.93%	21.16%	17.89%	28.05%	20.02%	17.61%
t	1.534	1.984	2.608	1.056	1.081	2.810
p	0.134	0.055	0.013	0.298	0.287	0.008*

Table 2. Percentage of excluded saccades for the retinitis pigmentosa (RP) and control groups, averaged over participants and trials. Note that the numbers seem surprisingly large. This is due to the exclusion criteria themselves, as an exclusion of one fixation outside of the image coordinates affects two (pre- and post-) saccades at once. The lower two rows show the results (*t*-test *t* and *p* values; Bonferroni-adjusted $\alpha = 0.008$) of the individual contrasts between RP- and control-group participants regarding the number of excluded saccades. *Notes*: $^{*}p =$ Bonferroni-adjusted $\alpha = 0.008$ applied due to multiple testing.

2003; Ramos Gameiro et al., 2017; Tatler, 2007). That means a strong/large central tendency described a very narrow central spatial bias, whereas a weak/small central tendency described a more expanded visual exploration of the whole image area. In contrast, the entropy captured the spatial bias as a general degree of the spread of fixations independent of geometric fixation patterns (Kaspar et al., 2013; Ramos Gameiro et al., 2017). Consequently, the central tendency and entropy captured two distinct approaches to examining the spatial distribution of fixations.

To quantify the spatial fixation bias in image space, we extracted the distribution of fixations in horizontal and vertical eccentricity respectively, separated for each participant and image size in both the scaled and the cropped condition. From these eccentricities we calculated the standard deviations, providing a measure of the extent of fixation distributions and thus the central tendency of fixations (Ramos Gameiro et al., 2017). Low standard deviations indicated a high central concentration of fixations and thus a strong central tendency. In contrast, high standard deviations indicated a higher distribution of fixations across the whole image and thus a weak central tendency (Figure 3a).

Note that the spatial fixation bias relies on specific geometric patterns of the distribution of fixations. That is, the central tendency qualifies only the density of fixations in the central image region. Entropy measures are independent of such geometric patterns. More precisely, entropy provides a measure of the disorderliness and thus heterogeneity of fixations in image space (Figure 3b). Hence, we used entropy as an additional measure to quantify the general spatial distribution of fixations in image space. We calculated fixation maps for each trial and participant by pooling all respective fixations in image space. Then we convolved the map of measured fixations with a Gaussian kernel with a full width at half maximum of 1° visual angle (Kaspar et al., 2013; Kaspar, Ramos Gameiro, & König, 2015; Ramos Gameiro et al., 2017). This approximately matches the size of the central part of the fovea. Next, the map was normalized to integral one, resulting in a fixation density map (FDM) estimating the probability of fixating a region of the stimulus. We calculated the entropy E at location x for participant p observing image i:

$$E(i,p) = -\sum \mathrm{FDM}(x,i,p) \times \log_2 \mathrm{FDM}(x,i,p). \quad (3)$$

Note that an FDM is strictly smaller than 1.0. This results in a negative logarithm. Hence, to get a positive entropy, we added a negative sign in Equation 3. However, entropy measures are sensitive to the sample size of the data (Hausser & Strimmer, 2009). In the domain of eye tracking, the number of fixations defines the sample size. Therefore, we applied a bootstrapping method with downsampling to calculate the entropy scores (Wilming, Betz, Kietzmann, & König, 2011). That means we randomly sampled nine valid fixations

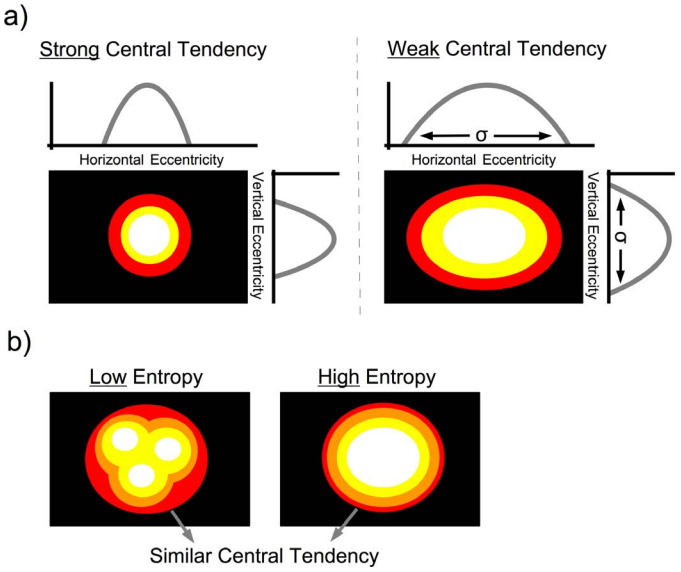

Figure 3. (a) Example showing a strong bias toward the center of the image and thus strong central tendency (left side). In contrast, a larger extent of the distribution of fixations leads to a weak central tendency (right side). We measured the central tendencies in horizontal and vertical eccentricity by calculating the standard deviation of the distribution of fixations. (b) Example of a homogenous spread of fixations leading to low entropy (left side). In contrast, a higher disorderliness of fixations (heterogeneity) leads to high entropy (right side). Note that entropy can differ although the central tendency stays similar (red circles).

made by the participant on a trial and calculated the entropy (downsampling). This process was repeated 500 times (bootstrapping). The final entropy for the corresponding participant and trial was then calculated by averaging the entropy scores obtained in the bootstrapping. We used nine fixations for downsampling to get the best trade-off of having reliable statistical power (Wilming et al., 2011) and excluding only a minimum number of trials that did not provide enough sampling data (excluded trials: 10.41% in data of control group; 5.46% in data of RP group).

As a result, higher entropy scores indicated a larger distribution of fixations and thus a smaller general spatial bias independent of geometric patterns.

Data analysis

For statistical analysis of the data, we used standard analyses of variance (ANOVAs) providing the significance level p as well as the effect size η_p^2. Post hoc comparisons (if needed) were done with paired t tests, with significance level p and effect size d'.

Differences between RP and control groups

In order to analyze differences of the variances in the dependent variables between the RP and control groups, we used an F test for equality of two variances (Senedecor & Cochran, 1989). The test indicates a significant difference between two variances if the resulting F,

$$F = \frac{s_1^2}{s_2^2}, \quad (4)$$

is smaller than the respective critical F_{low} or larger than the respective critical F_{high} boundaries:

$$F_{\text{low}} = F_{a/2,N_1-1,N_2-1} \quad (5)$$

and

$$F_{\text{high}} = F_{1-a/2,N_1-1,N_2-1} \quad (6)$$

(with N_1 and N_2 as number of participants and α as significance level, here $\alpha = 0.050$). The subscripts in Equations 5 and 6 refer to the corresponding alpha as well as the degrees of freedom ($N_1 - 1$, $N_2 - 1$) of the respective critical F distributions. Note that the F test for equality of two variances requires normality in the two sample populations being compared.

Data trends within RP participants with varying progress of the disease

For analyzing correlations and trends of the tested dependent variable and the degree of visual-field loss in RP participants, we used a standard linear regression with significance level p and correlation factor R^2. We did not use a nonlinear regression, in order to prevent overfitting. That is, RP participants with divergent characteristics in the dependent variables would highly influence such nonlinearity. Note that a linear regression requires normality in the respective residuals. Normality was tested with a standard Anderson–Darling test.

Analysis of the distribution of saccade amplitudes

Saccade amplitudes provided a further estimate of visual exploration by describing the distance between two consecutive fixations. Following our second hypothesis, we compared the distributions of saccades between the RP and control groups. For this, we analyzed frequency distributions of saccade amplitudes according to a previous study (Ramos Gameiro et al., 2017). That is, individually for each participant we sampled the saccades from 0° to 20° binned into steps of 0.5°. Then we divided the absolute frequencies of sampled saccades within each bin by the total number of saccades, resulting in probability distributions. For a statistical analysis, we compared the respective distribution of saccade amplitudes of individual RP participants with the respective distribution of individual healthy control participants with a chi-square test according to

$$\chi^2 = \sum_{i=1}^{\text{bins}} \left(\frac{\Delta\mu_i^2}{\Delta\sigma_i^2} \right), \quad (7)$$

with

$$\Delta\mu = \mu_{\text{dist1}} - \mu_{\text{dist2}} \quad (8)$$

and

$$\Delta\sigma = \sqrt{\frac{\sigma_{\text{dist1}}^2}{n} + \frac{\sigma_{\text{dist2}}^2}{n}}, \quad (9)$$

where n is the number of trials included in the respective saccade distribution, $\Delta\mu$ denotes the difference of means (averaged saccade distribution across trials of each participant) of the two saccade distributions (dist1 and dist2), and $\Delta\sigma$ denotes the respective overall variance of dist1 and dist2. We included the overall variance in order to weight the differences of frequencies in the compared distributions. Larger χ^2 values indicate a higher difference between the two distributions.

Results

Spatial fixation bias

Our first hypothesis stated that individuals with RP show an increased spatial bias due to strategic and

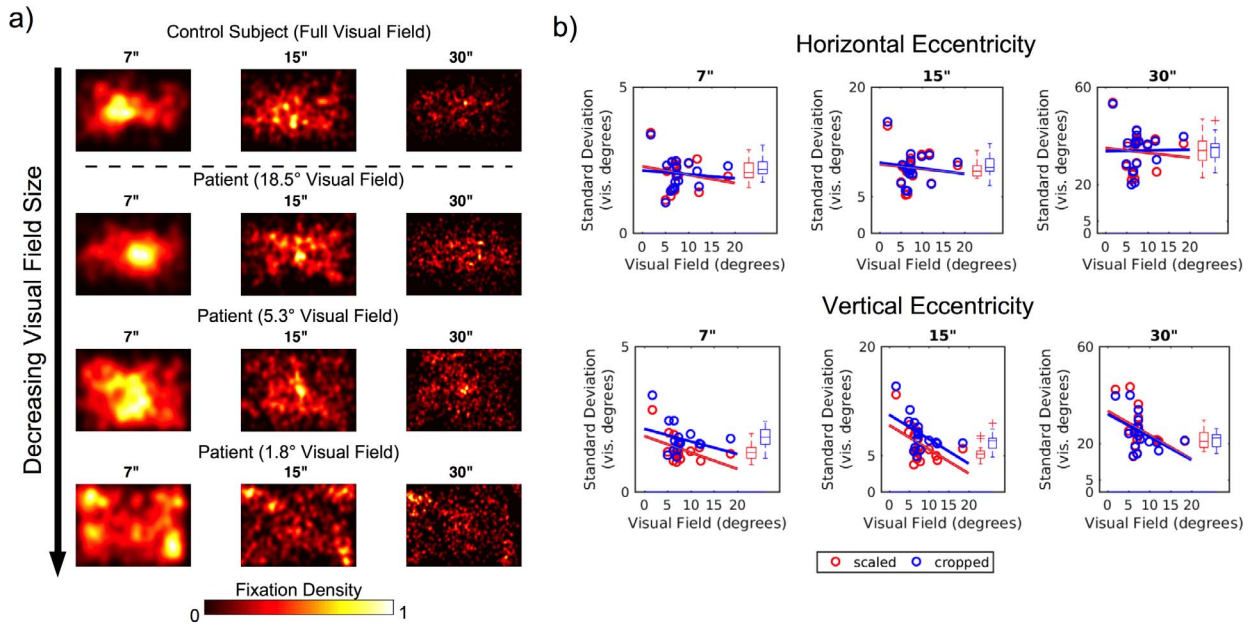

Figure 4. (a) Spatial distribution of fixations (fixation density map [FDM]) averaged over trials for each image size—here, for one example control participant (upper row) and three example participants with retinitis pigmentosa with consecutively decreasing visual field size. Note: To avoid an excess of figure panels, we presented FDMs of the scaled condition only. The corresponding FDMs of the cropped condition showed similar patterns. Also note that we normalized the different image sizes to one baseline in the panels (i.e., visual upscaling of 7- and 15-in. images to 30 in.) to provide better visualization and comparison of the FDMs. (b) Results of the central tendency as measured by the standard deviation of the distribution of fixations in horizontal (upper row) and vertical (lower row) eccentricity. Each circle represents the data of one individual with retinitis pigmentosa, sorted by visual-field size for the scaled (red) and cropped (blue) conditions. The box plots represent the averaged data of control participants for the scaled (red) and cropped (blue) conditions. Note: For better visualization of the data, the *y*-axis shows a different scaling across image sizes.

more active visual-search behavior. As a first step, we thus examined the general visual-search behavior of participants in the control and RP groups characterized by the spatial distribution of fixations. We calculated fixation density maps for each participant in both groups, individually for each of the three image sizes and separately for the scaled and cropped conditions (Figure 4a). Upon initial inspection of Figure 4a, we found a typical central spatial bias of fixations in control-group participants throughout all image sizes as well as in RP-group participants with early stages of the disease in small images. However, if image information exceeds the visual-field size of the observer (as indicated by a smaller visual field or larger image size), the central spatial bias expands toward peripheral areas of the image. Thus, individuals in the RP group showed distinct spatial biases dependent on their visual-field size and the image size.

For a statistical analysis of the spatial bias with respect to the central tendency, we separated the distribution of fixations by horizontal and vertical eccentricity and calculated the extent of these eccentricities as a function of standard deviation (see Methods). We compared the resulting standard deviations with a 2 (image condition: scaled, cropped) × 3 (image size: 7, 15, 30 in.) × 2 (subject group: control, RP) repeated-measures ANOVA (Greenhouse–Geisser corrected, due to violation of sphericity in all factors) for, respectively, horizontal and vertical eccentricity.

In horizontal eccentricity, results revealed a significant main effect on the central tendency of image size, $F(1.032, 36.106) = 800.703$, $p < 0.001$; $\eta_p^2 = 0.958$, indicating that larger images led to a reduced central tendency as shown by increasing standard deviations (Figure 4b). The ANOVA did not reveal any further significant effects, neither of image condition, all Fs $\leq$ 2.005, all ps $\geq$ 0.166, all η_p^2s $\leq$ 0.054, nor of subject group, $F(1, 35) = 0.056$, $p = 0.814$, $\eta_p^2 = 0.002$. However, note that the chance level of randomly assigning 30-in. images to either the scaled or the cropped condition might have led to an enhancement of false negatives (see Methods). The nonsignificance of image condition in this ANOVA might thus have related to a type 2 error. We therefore ran a separate 2 (image condition: scaled, cropped) × 2 (image size: 7, 15 in.) ANOVA excluding 30-in. images. The results indeed showed a significant difference between image conditions, $F(1, 35) = 7.277$, $p < 0.050$, $\eta_p^2 = 0.172$, indicating that scaled images had a stronger horizontal central tendency (mean = 5.47°) than cropped images (mean = 5.63°). Most importantly, as indicated by the initial 2 × 3 ANOVA on a group level, there is no

statistical difference in the central tendency on horizontal eccentricity between the control and RP groups.

In vertical eccentricity, results also revealed a significant main effect of image size, $F(1.041, 36.444) = 529.289$, $p < 0.001$, $\eta_p^2 = 0.938$. In addition, we found a significant main effect of image condition, $F(1.000, 35.000) = 9.889$, $p < 0.005$, $\eta_p^2 = 0.220$, showing that scaled images led to a stronger vertical central tendency (all image sizes: $M = 10.29°$; excluding 30-in. images: $M = 3.65°$) than cropped images (all image sizes: $M = 10.69°$; excluding 30-in. images: $M = 4.63°$). Further, the results revealed a significant Image size × Image condition interaction, $F(1.126, 39.420) = 27.249$, $p < 0.001$, $\eta_p^2 = 0.438$. Paired t tests (Bonferroni-adjusted $\alpha = 0.008$) showed that the central tendency in vertical eccentricity increased with image size in both image conditions, all $t(36) \geq 17.418$, all ps < 0.001. Thus, the significant interaction reflected different effect sizes according to changes in the image size (Figure 4b). We found no main effect of subject group, $F(1, 35) = 3.660$, $p = 0.064$, $\eta_p^2 = 0.095$, nor an Image size × Subject group interaction, $F(129.886, 1235.305) = 3.680$, $p = 0.061$, $\eta_p^2 = 0.095$, nor any further effects, all Fs ≤ 0.886, all ps ≥ 0.353, all η_p^2s ≤ 0.025. Taken together, we found no difference in the central tendency between RP- and control-group participants on the group level, neither in horizontal nor vertical eccentricity.

Interestingly, close inspection of Figure 4b indicates that individual RP participants showed higher variances in their individual central tendencies (i.e., standard deviations) as compared to control participants. For a formal analysis of the difference between the variances of both participant groups, we used an F test for equality of two variances. We first calculated the F test of variances in horizontal eccentricity. Normality was given in all sample populations (Anderson–Darling test; all ps ≥ 0.079; Razali & Wah, 2011). The F test could thus be applied to compare the sample variances of control- and RP-group participants for all image sizes in the scaled and cropped conditions. Recall that significance in this F test was a measure of boundaries (see Methods). That is, if the F value was outside the corresponding boundaries F_{low} and F_{high}, the two tested variances were significantly distinct at $\alpha = 0.050$. The results revealed that the variance of the central tendencies was significantly different between the RP group and the control group in scaled 15- and 30-in. images and cropped 30-in. images—scaled 15 in.: $F = 4.639$, $F_{low} = 0.376$, and $F_{high} = 2.892$; scaled 30 in.: $F = 2.083$, $F_{low} = 0.437$, $F_{high} = 1.997$; cropped 30 in.: $F = 2.572$, $F_{low} = 0.437$, $F_{high} = 2.001$. No further results were found: all $F_{low} = (0.385, 0.236, 0.379) < F = (2.818, 3.113, 2.514) < F_{high} = (22.637, 24.194, 2.836)$.

In vertical eccentricity, normality was given in all sample populations (Anderson–Darling test; all ps ≥ 0.068), except for the RP group with scaled 7- and 30-in. images and cropped 7-in. images (Anderson–Darling test; all ps < 0.050). Therefore, we could only apply the F test to compare the sample variances of the control and RP groups with scaled 15-in. images and cropped 15- and 30-in. images. The results showed that the variance of central tendencies was different between groups in scaled 15-in. images and cropped 15- and 30-in. images—scaled 15 in.: $F = 6.108$, $F_{low} = 0.369$, $F_{high} = 3.042$; cropped 15 in.: $F = 3.681$, $F_{low} = 0.376$, $F_{high} = 2.909$; cropped 30 in.: $F = 5.786$, $F_{low} = 0.428$, $F_{high} = 2.096$. In general, we found that RP participants showed larger variances on large images compared to control participants. Inspection of the individual RP participants' data indicated that each participant showed almost identical results of central tendency in scaled and cropped images (Figure 4b). This suggests that individual RP participants maintained similar visual behavior in the scaled and cropped conditions. Thus, RP participants showed reproducible individual differences in central tendency.

In order to get into more detail concerning the large differences of individual central tendencies in RP participants, we focused on the dependence of the change in central tendency on residual visual-field size. In the following analysis, we thus only used the data of RP participants, and applied linear regressions separately for the horizontal and vertical eccentricity for the scaled and cropped conditions and for each image size. In horizontal eccentricity, we did not find significant effects (all ps ≥ 0.483, all R^2s ≤ 0.033). Normality was given in the residuals of all tested linear models (Anderson–Darling test; all ps ≥ 0.112). Hence, in horizontal eccentricity the central tendency showed no dependence on visual field size. In vertical eccentricity, results revealed a significant effect in scaled and cropped 15-in. images (both ps ≤ 0.037, both R^2s ≥ 0.259), showing reduced standard deviations (i.e., an increase of central tendency) with an increase of the visual-field size (Figure 4b). The linear regression of scaled and cropped 7- and 30-in. images turned out to be not significant (all ps ≥ 0.077, R^2s ≤ 0.194). Normality was given in the residuals of all tested linear models (Anderson–Darling test; all ps ≥ 0.119). Hence, in vertical eccentricity we found that RP participants with smaller visual-field sizes had a decreased central tendency—that is, larger variance—for the 15-in. images.

To conclude, we found that spatial bias, as indicated by central tendency, was not different between control- and RP-group participants on a group level. However, in vertical eccentricity, a reduced visual field led to a reduced central tendency in 15-in. images and thus a larger spatial bias. Further, we saw that RP participants developed individual differences in large images, providing personalized central tendencies.

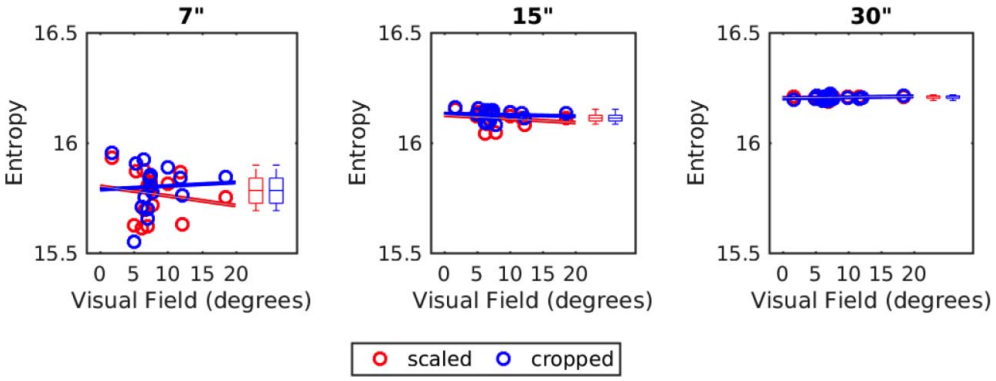

Figure 5. Disorderliness of fixations as measured by entropy. Each circle represents the data of one participant with retinitis pigmentosa, sorted by visual-field size for the scaled (red) and cropped (blue) conditions. The box plots represent the averaged data of control participants for the scaled (red) and cropped (blue) conditions.

For a further analysis of spatial bias, we calculated entropy. Entropy measures the distribution of fixations independent of geometric clusters and thus gives another view of the general visual behavior. We extracted the entropy scores of control- and RP-group participants for each image size in the scaled and cropped conditions and calculated a 2 (image condition) × 3 (image size) × 2 (subject group) repeated-measures ANOVA (Greenhouse–Geisser corrected, due to violation of sphericity in all factors). The results revealed a main effect of image size, $F(1.078, 37.725) = 1036.691$, $p < 0.001$, $\eta_p^2 = 0.967$, showing a general increase of entropy with increasing image size (Figure 5). Furthermore, we found a significant main effect of image condition, $F(1, 35) = 44.820$, $p < 0.001$, $\eta_p^2 = 0.562$, showing that entropy was smaller in scaled images (all image sizes: $M = 16.03$; excluding 30-in. images: $M = 15.94$) than in cropped images (all image sizes: $M = 16.05$; excluding 30-in. images: $M = 16.17$). The results also revealed an Image size × Image condition interaction, $F(1.164, 40.754) = 27.707$, $p < 0.001$, $\eta_p^2 = 0.442$. Paired t tests (Bonferroni-adjusted $\alpha = 0.008$) showed that entropy increased with image size in both image conditions, all $t(36) \geq 25.748$, all ps < 0.001. Thus, the significant interaction reflected different effect sizes according to changes in the image size. No further effects were revealed, most importantly including no effect of subject group, all Fs ≤ 3.649, all ps ≥ 0.064, all η_p^2s ≤ 0.094. Hence, we did not find a difference in entropy between control- and RP-group participants.

Using the F test for equality of two variances, we again tested whether RP participants showed larger individual differences compared to control participants. Normality was given in the sample populations in all image conditions and image sizes (Anderson–Darling test; all ps ≥ 0.144), except for scaled 15- and 30-in. images and cropped 30-in. images (Anderson–Darling test; all ps < 0.050). We thus could use the F test only with scaled 7-in. as well as cropped 7- and 15-in. images. However, the results turned out to be significant only for cropped 7-in. images: $F = 4.396$, $F_{low} = 0.382$, $F_{high} = 2.777$. No further effects were found: all $F_{low} = (0.382, 0.383, 0.330) < F = (2.516, 1.307, 1.269) < F_{high} = (2.778, 2.760, 2.755)$. Hence, in general, RP participants tended to show individual preferences of entropy only in small images, not large.

To further analyze whether the entropy depended on the visual-field size of RP participants, we applied a linear regression to all image sizes in the scaled and cropped conditions. The results revealed no significant correlation between entropy and visual-field size in any of the image sizes or image conditions, all ps ≥ 0.435, all R^2s ≤ 0.041. Normality was given in the residuals of all linear models tested (Anderson–Darling test; all ps ≥ 0.058), except for scaled and cropped 15-in. images (Anderson–Darling test; all ps < 0.050). Taken together, a varying visual-field size did not lead to a change in entropy. To conclude, RP participants did not adapt their spatial bias, as measured by entropy, dependent on individual visual-field size.

In summary, the results of the central tendency and entropy only partly supported our first hypothesis. Instead of a general difference in spatial bias between RP- and control-group participants, we observed only individual differences in the extent of the RP participants' central tendencies in large images and entropy in small images.

Saccade amplitudes

In our second hypothesis, we stated that saccade amplitudes of RP participants will not adapt to a reduced visual-field size. Thus, in the following we extracted saccade amplitudes and analyzed at which distance subsequent fixations in visual search were made. We extracted the mean saccade amplitude for each participant individually for each image size in the

scaled and cropped conditions and calculated a 2 (image condition) × 3 (image size) × 2 (subject group) repeated-measures ANOVA (Greenhouse–Geisser corrected, due to violation of sphericity in image size). The results revealed a main effect of image size, $F(1.143, 39.992) = 744.896$, $p < 0.001$, $\eta_p^2 = 0.955$, showing an increase of the mean saccade amplitude in large images (Figure 6a). Further, we found a significant main effect of image condition, $F(1, 35) = 38.678$, $p < 0.001$, $\eta_p^2 = 0.525$, showing that saccade amplitudes were smaller in scaled images (all image sizes: $M = 4.51°$; excluding 30-in. images: $M = 3.27°$) than in cropped images (all image sizes: $M = 4.66°$; excluding 30-in. images: $M = 3.52°$). The results also revealed an Image size × Image condition interaction, $F(1.971, 68.997) = 30.651$, $p < 0.001$, $\eta_p^2 = 0.467$. Paired t tests (Bonferroni-adjusted $\alpha = 0.008$) showed that saccade amplitudes increased with image size in both image conditions, all $t(36) \geq 21.361$, all ps < 0.001. Thus, the significant interaction reflected different effect sizes of image size. No further effects were found, including no significant effect of subject group, all Fs ≤ 1.060, all ps ≥ 0.310, all $\eta_p^2 \leq 0.029$ (Figure 6a). Hence, the control and RP groups did not show differences in mean saccade amplitudes on a group level.

Next, we analyzed whether RP participants showed individual differences depending on their impaired visual-field size. Therefore, similar to our previous analysis, we calculated an F test for equality of two variances. Normality was given in the sample populations of all image sizes in the scaled and cropped conditions (Anderson–Darling test; all ps ≥ 0.231), such that we could compute the F test across all conditions. However, the results revealed no significant differences in any of the image sizes in the scaled condition—all $F_{low} = (0.235, 0.306, 0.343) < F = (1.943, 3.032, 2.313) < F_{high} = (2.533, 5.958, 3.841)$—or the cropped condition—all $F_{low} = (0.248, 0.311, 0.341) < F = (2.598, 2.109, 1.954) < F_{high} = (1.722, 5.443, 3.926$; see Figure 6a). Hence, the variance of RP participants did not differ from that of control participants. We also applied a linear regression to the RP-participant data for each image size in the scaled and the cropped condition. But again, we did not find a significant correlation of visual-field size and mean saccade amplitude, all ps ≥ 0.238, all R^2s ≤ 0.092 (Figure 6a). Normality was given in the residuals of all tested linear models (Anderson–Darling test; all ps ≥ 0.323). To conclude, our data revealed that an impaired visual-field size did not affect mean saccade amplitude.

Our previous results revealed no adaptation of averaged saccade amplitude with respect to a reduced visual field. However, the calculated mean amplitudes could have underlay individual distributions of saccade amplitudes. In the next step, therefore, we compared the distribution of saccade amplitudes of RP- and control-group participants.

We calculated the distribution of saccade amplitudes for each RP- and control-group participant individually for each image size and separated the scaled and cropped conditions. An initial inspection revealed that RP participants indeed showed individual distributions of saccade amplitudes compared to control-group participants (Figure 6b). With chi-square tests, we compared the calculated distributions with each other, resulting in a 2-D color matrix with four quadrants: Quadrant 1 is a comparison of saccade distribution within control-group participants; quadrant 2 compares between control- and RP-group participants; quadrant 3 shows the same data as quadrant 2 (the matrix is symmetric); and quadrant 4 is a comparison within RP participants. As indicated by generally larger χ^2 values, Figure 6c reveals that the distributions of saccade amplitudes in individuals with RP grew more distinct from those in control-group participants and from each other's with increasing image size (quadrants 2/3 and 4, respectively), whereas control-group participants revealed more similar saccade distributions (quadrant 1). These results suggest that RP participants tended to distribute saccade amplitudes more individually on large images as compared to control-group participants.

Next, we investigated how these individual differences occurred and examined whether RP participants visually restricted their visual search to their visual field or also searched in blind areas. To test this, we proposed a model based on control-group participants, simulating the probability that saccade amplitudes fall into a specific visual-field size. The goal of the simulation model was to provide an additional view on how saccade amplitudes were distributed in control-group participants in order to compare it with the saccadic behavior of RP participants. We included only data of control-group participants. We sampled all saccade amplitudes from 0° to 20° (sampling range), binned in steps of 0.5°, and then calculated a cumulative distribution function. Particularly, we calculated the relative frequency of saccades amplitudes of the respective bin and cumulated these frequencies consecutively from smallest to largest bin in the sampling range. The resulting function provided a simulation curve showing the probability of saccade amplitudes (Figure 6d). In a second step, we focused on the data of individual RP participants. For each RP participant, we summed up the number of saccades with amplitudes that were smaller than the respective visual-field size. The frequencies were normalized by dividing the number of sampled saccades by the number of all saccades the participant made. The resulting number provided a probability that saccades fell into the participant's visual field (Figure 6d).

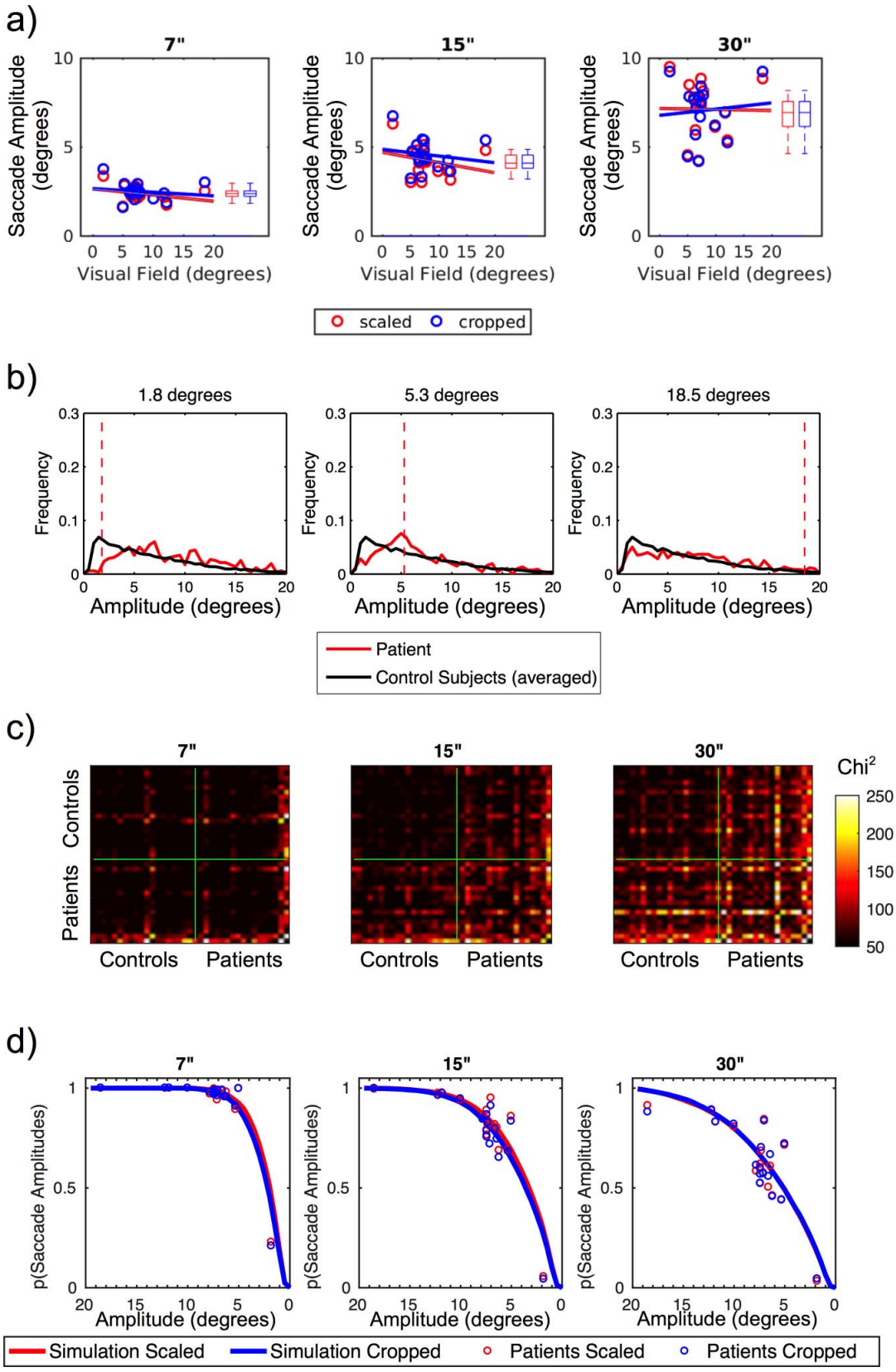

Figure 6. (a) Mean saccade amplitudes. Each circle represents the data of one participant with retinitis pigmentosa (RP), sorted visual-field size for the scaled (red) and cropped (blue) conditions. The box plots represent the averaged data of control participants for the scaled (red) and cropped (blue) conditions. (b) Distribution of saccade amplitudes for three example RP participants with continuously increasing visual-field size (red line), in comparison with the averaged distribution of saccade amplitudes of control

→

←

participants (black line). The vertical red dotted line indicates the visual-field size of the respective RP participant. (c) 2-D color matrix showing the individual comparisons of the distribution of saccade amplitudes between all RP- and control-group participants (as specified in Results). Each row represents an individual participant, ordered by group. Columns are a symmetric projection of the rows. Thus, each voxel of the color matrix shows the difference of the averaged saccade distribution between two participants. Lighter colors represent higher χ^2 values and thus greater difference in the two compared saccade distributions. RP participants are sorted by visual-field size, from large to small. (d) Simulated cumulative distribution function based on healthy control participants for the scaled (red line) and cropped (blue line) condition. Each circle represents the data of one RP patient sorted by his/her respective visual field size (from large to small) for the scaled (red) and cropped (blue) conditions.

Inspection of Figure 6d reveals that the calculated probabilities of RP participants with respect to their visual-field size adequately followed the curve of the simulation model in all image sizes and in both scaled and cropped conditions. This suggests that RP participants did not adapt saccadic behavior to their specific visual-field size, with the result that saccades have a higher probability of ending outside the visual field—a "blind search"—in individuals with RP who have severe loss of peripheral vision.

Taken together, even though the mean of saccade amplitudes was similar in participants in both the RP and control groups, we found individual differences of the distribution of saccades in RP participants on large images. However, these differences did not reflect an adaptation of saccade amplitudes to visual-field size, and consequently they resulted in a high probability of visual search in the blind visual field. Overall, these results supported our second hypothesis.

Number of fixations and fixation duration

In the following analysis, we addressed our third hypothesis, relating to the number of single fixations affected by a distinct strategic viewing behavior as shown by differences in the central tendency and distribution of saccade amplitudes in individuals with RP. We thus extracted the number of fixations individually for each RP- and control-group participant, separated for each image size and image condition. Then we calculated a 2 (image condition) × 3 (image size) × 2 (subject group) repeated-measures ANOVA (Greenhouse–Geisser corrected, due to violation of sphericity in image size). The results revealed a main effect of image size, $F(1.579, 55.280) = 244.318$, $p < 0.001$, $\eta_p^2 = 0.875$, showing an increase of the number of fixations in large images. We further found a significant main effect of image condition, $F(1, 35) = 14.677$, $p < 0.005$, $\eta_p^2 = 0.295$, showing that fewer fixations were made in scaled images (all image sizes: $M = 16.93$; excluding 30-in. images: $M = 15.88$) than in cropped images (all image sizes: $M = 17.23$; excluding 30-in. images: $M = 16.31$). The results also revealed an Image condition × Image size interaction, $F(1.927, 67.428) = 3.435$, $p < 0.050$, $\eta_p^2 = 0.089$. Paired t tests (Bonferroni-adjusted $\alpha = 0.008$) showed that the number of fixations increased with image size in both image conditions, all $t(36) \geq 6.864$, all ps < 0.001. Thus, the significant interaction reflected different effect sizes according to changes in the image size. We did not find a significant main effect of subject group, $F(1, 35) = 3.969$, $p = 0.054$, $\eta_p^2 = 0.102$ (Figure 7a), nor any further effects, all Fs ≤ 2.776, all ps ≥ 0.083, all $\eta_p^2 \leq .073$. Hence, RP participants did not differ statistically from control-group participants in number of fixations.

We again calculated an F test for equality of two variances, to analyze whether RP participants showed individual differences depending on their impaired visual-field size. Normality was given in the sample populations of all image sizes in the scaled and cropped conditions (Anderson–Darling test; all ps ≥ 0.379). Consequently, we could compute the F test across all conditions. However, the results revealed no significant differences by image size in the scaled condition—all $F_{low} = (0.396, 0.401, 0.405) < F = (1.060, 1.141, 0.857) < F_{high} = (2.523, 2.441, 2.385)$—or the cropped condition—all $F_{low} = (0.391, 0.404, 0.405) < F = (0.777, 0.819, 1.045) < F_{high} = (2.539, 2.402, 2.385$; see Figure 7a). Hence, the sample variance of RP participants did not differ from that of control-group participants. We also applied a linear regression to the RP-participant data in each image size for the scaled and cropped conditions; however, correlation results turned out to be nonsignificant, all ps ≥ 0.125, all R^2s ≤ 0.15. Normality was given in the residuals of all tested linear models (Anderson–Darling test; all ps ≥ 0.358). Taken together, our data do not provide statistical evidence to claim that the number of fixations differed between RP- and control-group participants.

Next, we focused on single fixation duration as a consequence of a constant interplay between visual exploration, as indicated by the number of fixations, and visual information processing, as indicated by single fixation durations. We extracted the mean fixation duration individually for each participant, separated by image size, and calculated a 2 (image condition) × 3 (image size) × 2 (subject group)

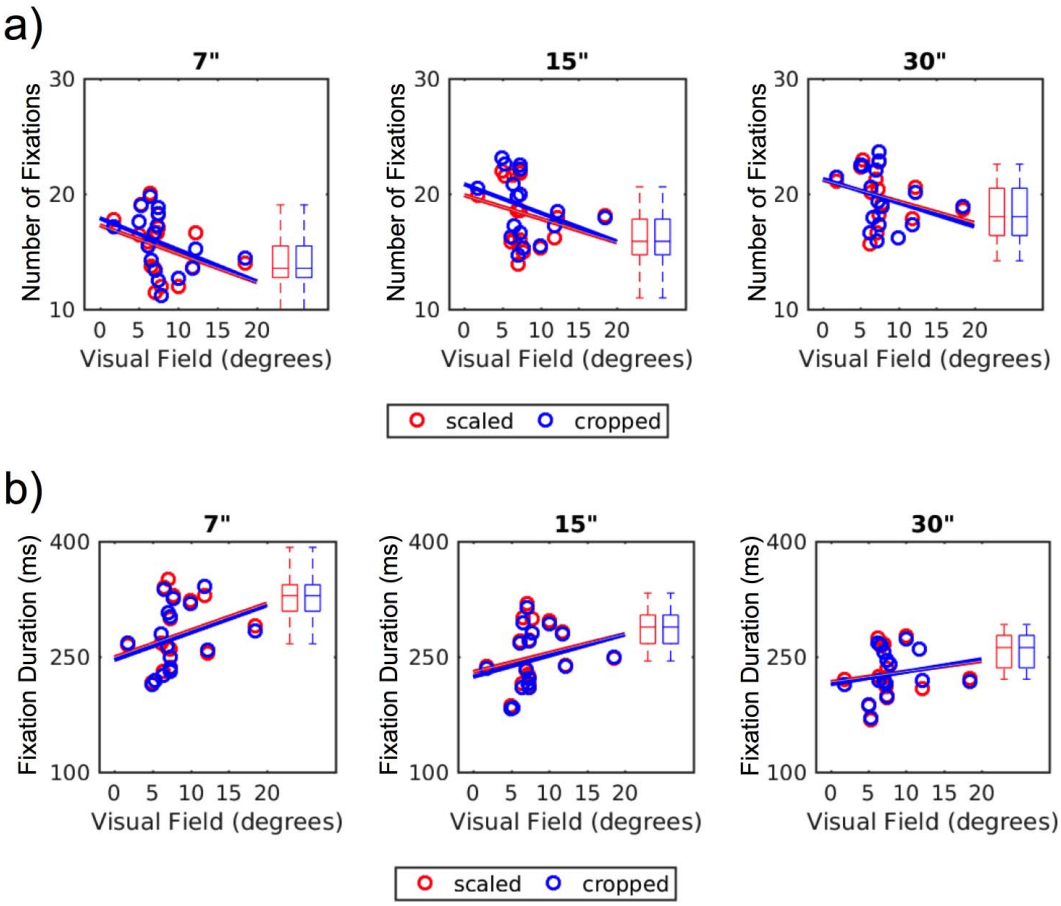

Figure 7. (a) Number of fixations; (b) single fixation durations. Each circle represents the data of one participant with retinitis pigmentosa, sorted by visual-field size for the scaled (red) and cropped (blue) conditions. The box plots represent the averaged data of control-group participants for the scaled (red) and cropped (blue) conditions.

repeated-measures ANOVA (Greenhouse–Geisser corrected, due to violation of sphericity in image size). The results revealed a main effect of image size, $F(1.336, 46.770) = 272.204$, $p < 0.001$, $\eta_p^2 = 0.886$, showing a decrease of fixation durations in large images (Figure 7b). We further found a significant main effect of image condition, $F(1, 35) = 17.561$, $p < 0.001$, $\eta_p^2 = 0.334$, indicating lower fixation durations in cropped images (all image sizes: $M = 266.69$ ms; excluding 30-in. images: $M = 279.34$ ms) than scaled images (all image sizes: $M = 270.79$ ms; excluding 30-in. images: $M = 284.74$ ms). Most importantly, results revealed a main effect of subject group, $F(1, 35) = 12.839$, $p < 0.005$, $\eta_p^2 = 0.268$, showing that RP participants in general had shorter fixation durations (250.26 ms) than control-group participants (287.23 ms). We also found a Subject group × Image size interaction, $F(1.336, 46.770) = 5.427$, $p < 0.050$, $\eta_p^2 = 0.134$. However, paired t tests (Bonferroni-adjusted $\alpha = 0.008$) showed that fixation durations decreased with increasing image size in the both subject groups—RP: all $t(16) \geq 4.931$, all $ps < 0.001$; control: all $t(19) \geq 14.396$, all $ps < 0.001$. Thus, the significant interaction reflected different effect sizes according to changes in the image size (Figure 7b). No further effects were found, all $Fs \leq 2.685$, all $ps \geq 0.080$, all $\eta_p^2 \leq 0.071$. Hence, RP participants had lower fixation durations than control-group participants, resulting in reduced depth of visual information processing.

Again, we calculated an F test for equality of two variances, to analyze whether RP participants showed individual differences depending on their impaired visual-field size. Normality was given in the sample populations of all image sizes in the scaled and cropped conditions (Anderson–Darling test; all $ps \geq 0.193$). We thus could compute the F test across all conditions. In the scaled condition, results revealed a significant difference of sample variances in images at 7 and 15 in.—7 in.: $F = 2.293$, $F_{low} = 0.463$, $F_{high} = 1.768$; 15 in.: $F = 2.844$, $F_{low} = 0.463$, $F_{high} = 1.772$—but not at 30 in.: $F_{low} = 0.462 < F = 1.765 < F_{high} = 1.778$. In the cropped condition, results revealed a significant difference of sample variances only in 7-in. images—$F = 2.208$, $F_{low} = 0.463$, $F_{high} = 1.769$—not in 15- or 30-in. images: both $F_{low} = (0.463, 0.462) < F = (1.699, 1.634) < F_{high} = (1.773, 1.779)$. Note here that each RP

participant showed almost identical results when their respective fixation durations in scaled and cropped images were compared (Figure 7b). This suggests that the results of the F test relied on consistent visual behavior and did not originate from random factors. Hence, RP participants showed higher individual differences according to fixation duration in small images.

We also applied a linear regression to the RP-participant data for each image size in the scaled and cropped conditions. However, although Figure 7b shows a decrease of fixation duration with decreasing visual field, correlation results turned out to be nonsignificant, all ps ≥ 0.231, all R^2s ≤ 0.094. Normality was given in the residuals of all tested linear models (Anderson–Darling test; all ps ≥ 0.082). Hence, we did not find a correlation between fixation duration and visual-field size for RP participants.

Taken together, we found that on average RP participants had lower fixation durations than control participants. Although we could not claim a correlation, we saw that RP participants exhibited individual differences in their own visual information processing, as shown by larger sample variances.

In general, results of the number and single duration of fixations partly supported our third hypothesis. We saw that RP participants with reduced peripheral vision did not change exploration, as indicated by a distinct number of fixations. However, visual information processing still decreased, as indicated by lower fixation durations.

Discussion

We investigated to what extent a gradual continuous loss of peripheral vision in individuals with RP affects natural visual behavior. We compared eye-movement behavior between participants with and without RP for different image sizes and different image conditions.

On spatial bias, we did not find a difference between RP- and control-group participants, as shown by central tendency and entropy. However, we saw that RP participants exhibited individual differences in the extent of their central tendencies with large images and entropy with small images. These results only partly supported our first hypothesis. On mean saccade amplitudes, we again did not find a difference between RP- and control-group participants. By examining the frequency distribution of saccade amplitudes, we found individual differences in RP participants for large images; however, these differences did not reflect an adaptation of saccade amplitudes to visual-field size. As a consequence, RP participants showed a high probability of visual search in the blind area of their visual field. These results fully supported our second hypothesis. On number of fixations, we saw that RP participants with reduced peripheral vision did not change exploration; however, visual information processing decreased, as indicated by lower fixation durations. These results partly supported our third hypothesis. Overall, the RP and control groups did not differ on group level in their natural visual behavior in most of the investigated oculomotor parameters.

With respect to spatial bias, RP participants only partly adapted visual-search behavior in favor of a more strategic viewing behavior. Visual exploration in terms of spatial bias did not differ between the two groups on a group level. This was evident for central tendency as well as for entropy measuring the heterogeneous spread of fixations. However, we found that the variance of individual differences in central tendency for large images across RP participants was higher than across control-group participants. This suggests that each individual developed their own strategy during the process of the disease. In addition, the loss of peripheral vision does not necessarily lead to a precisely circular visual field (Grover, 1998). Thus, spatial differences in peripheral visual loss could be a reason to develop individual strategies in viewing behavior. Further, our results showed that a severe loss of peripheral vision led to a reduced central tendency of midsize images in vertical eccentricity. As we presented natural images as stimuli, a possible explanation why the spatial bias changed only in vertical eccentricity could rely on human preferences in visual navigation in the environment. Previous studies have demonstrated that environmental structures led people to shift the central spatial bias (Foulsham, Walker, & Kingstone, 2011; Tatler, 2007)—for example, toward lower parts of images in interior natural scenes and upper parts in exterior natural scenes (Parkhurst & Niebur, 2003). For individuals with RP, the effect of environmental structures might be even more important—for example, in order to follow a road on the ground while keeping track of the scenery ahead. Hence, it seems to be more crucial for behavior to extend vertical rather than horizontal eye movements. Overall, on a group level the averaged spatial bias of RP participants did not differ from healthy visual behavior. However, with respect to the individual differences in spatial bias among RP participants, our results partly supported our first hypothesis that individuals with RP use a more strategic individual viewing behavior.

Furthermore, our results revealed that RP participants also did not adapt their visual behavior, as reflected by saccade amplitudes. In general, the mean saccadic amplitudes were not different between our two groups. These results are supported by a previous report of missing adaptation of saccadic behavior in tunnel vision (Luo et al., 2008). One potential reason

might rely on stable motor constraints in the saccadic system (Tatler, 2007) that lead humans to distribute saccade amplitudes in a log-normal shape with a magnitude of up to 15° visual angle (Gajewski et al., 2004; Pelz & Canosa, 2001; Tatler, 2007; Tatler et al., 2006). We assumed that these constraints were still robust in individuals with RP, such that no unified adaptation in saccadic behavior was initiated even though our results revealed reproducible individual differences of the distribution of saccades in RP participants on large images. As a consequence of the sustained saccade amplitudes, we saw that RP participants with moderate and severe peripheral visual-field loss often targeted saccades into blind areas of the retina. Overall, this supports our second hypothesis—that peripheral visual-field loss in RP does not lead to an adaptation of saccade amplitudes. Thus, in RP participants, many saccades were made into blind areas of the visual field, leading to a blind visual exploration.

For a better understanding of the individual search strategies of RP participants, we also examined the number and duration of fixations. We again saw that RP participants did not differ from control-group participants in terms of number of fixations. Hence, visual exploration as a measure of single fixations did not adapt to reduced visual fields. Nevertheless, fixation durations decreased in RP participants with loss of peripheral vision. In the literature, fixation durations are described as a measure for visual information processing (Unema et al., 2005). Consequently, as inferred from the present study, RP participants had reduced information processing for natural viewing behavior of small images. Again, they had larger variance in fixation durations than control-group participants with small and midsize images, indicating individual differences in visual information processing. We assume that RP participants could not risk reducing fixation durations in large images even further, as fixation durations cannot go below a certain threshold for conscious information processing (van Diepen, De Graef, & D'Ydewalle, 1995). Hence, individual differences as indicated by larger variance in RP participants occurred only with small and midsize images.

Furthermore, we found general main effects of image size and condition in both participant groups. With respect to the different image sizes and image conditions tested in this study, we could replicate the results of our previous study showing that large images led to enhanced exploration in healthy participants (Ramos Gameiro et al., 2017). The increase of exploration was shown by a reduced central tendency with higher entropy and longer mean saccade amplitudes. The number of fixations also increased, consequently reducing fixation durations and thus visual information processing (Ramos Gameiro et al., 2017). As mentioned, these effects were found in both tested participant groups in the present study, showing that image size played a crucial role in the adaptive visual behavior of RP participants. Although we found statistical differences between the scaled and cropped conditions in all independent variables, the general effects of adapted visual behavior according to image size applied to both conditions. In fact, we saw that the differences between scaled and cropped conditions followed only weak characteristics. However—and more importantly—we found similar trends between the two conditions of image manipulation, and thus showed that image size as an isolated factor affected our dependent variables. That is, the adaptation of visual behavior with different image sizes only weakly relied on side factors, such as a varying depth of details of local objects within the image scenes. Again, this was also shown in healthy subjects in our previous study (Ramos Gameiro et al., 2017). Thus, by replicating our previous findings we underline the robustness of the study design and its appropriateness for the investigation of natural viewing behavior.

There were a number of limitations of the present study. We have to consider that more eye-tracking parameters should be examined in order to fully understand the extent of individual visual-behavior differences of people with RP. One approach could be to compare whole scan paths on individual images between individuals with and without RP. However, recent literature has described comparison between only two scan paths (Cristino, Mathôt, Theeuwes, & Gilchrist, 2010; Dewhurst et al., 2012). Hence, scan-path analyses in large data sets with more than two comparisons are complicated and need a new tier of data processing without a generally accepted standard. Thus, this approach is beyond the scope of the present study. In addition, visual behavior in natural environments is a combination of eye and head movements. Individuals with RP could learn certain viewing strategies that highly involve head movements and require only slight adaptations in eye movements. In our study, similarly to typical eye-tracking studies (Kaspar et al., 2013; Ramos Gameiro et al., 2017; Wilming et al., 2017), we verbally instructed our participants not to move their head during recordings. Especially on large images, this verbally instructed restriction of head movements could have limited learned viewing strategies of participants with RP. Further studies should focus on visual behavior as an interplay between head and eye movements, providing eye-tracking measures in virtual environments or the real world.

An issue of importance that has to be considered in our study is the amount of data obtained from participants with RP. Most of our RP participants had visual-field sizes ranging between 5° and 10° visual

angle, which were thus larger than the majority of saccadic amplitudes. Only a few had already severe loss (1.8° visual angle) or healthylike vision (18.5° visual angle). This limited our analyses with respect to detailed claims of correlation processes between visual-field size and adaptation of eye movements. In addition, our control-group participants were mostly young adults, whereas our RP participants were generally older. While these age differences might have a potential effect on the obtained results—for example, in terms of strategic viewing behavior (Gruber et al., 2014) and information processing as reflected by fixation durations (McPhee, Scialfa, Dennis, Ho, & Caird, 2004)—we did not observe general statistical differences between the two groups. Consequently, although age differences in visual behavior have to be taken into consideration, they apparently did not have a relevant impact on the present study. For a more detailed account, however, a larger number of patients with similar age as controls but a higher variety of visual-field sizes should be tested in future studies.

With regard to the present study, we concluded that individuals with RP mostly maintained healthy visual behavior, adapting only some aspects. As shown, even though the visual fields of individuals with RP were reduced, the explorative behavior stayed similar and thus led to a blind search as saccades were targeted outside of the visual field. Because a reduced visual field also leads to decreased covert attention, we assumed other influences than the interplay of overt and covert attention for this sustained visual behavior. Although peripheral cues guide saccade planning and thus exploration, studies have shown that even in free viewing, top-down information highly affects where to look next (Itti & Koch, 2001; Kowler, 2011). According to the relevance and interpretation of objects in a scenery, attention might rely even more on top-down information than on visual salience (Kietzmann, Geuter, & König, 2011; Kietzmann & König, 2015; Land, 2009). We assumed therefore that individuals with RP relied on such top-down information in visual behavior.

RP is a disease that often follows a constant but slow degenerative process over the course of several years (Berson et al., 1985; Hamel, 2006). During that time, individuals might train unconsciously to use top-down information rather than rely on salient bottom-up information when deciding where to look next. In this regard, Açık, Sarwary, Schultze-Kraft, Onat, and König (2010) have found that older adults usually use top-down information in visual search, whereas young adults rely on bottom-up information. Thus, relating back to the age difference between generally younger control-group participants and older RP participants in our study, the tendency to favor top-down rather than bottom-up search in visual processing might even be more pronounced. Additionally, in natural environments certain structures and shapes repeat and follow typical progression. Using this knowledge could help to predict and expect certain objects in the periphery while exploring a scene (Shinoda, Hayhoe, & Shrivastava, 2001). Consequently, we assume that top-down information played a large role for individuals with RP that helped to maintain similar explorative behavior as control-group participants. However, although top-down knowledge could help to process peripheral objects, individuals with RP might still lack in overall understanding of the scene context. Hence, those with visual-field loss might have a stronger necessity to sample the overall scene context, which might be related to the less pronounced ability to process single fixated regions in full depth. This leads to reduced in-depth information processing and thus reduced fixation durations as compared to healthy controls. Overall, individuals with RP appear to rely on top-down knowledge to guide visual attention as an adaptation to the reduced input of the peripheral visual field, resulting in visual exploration that follows healthylike behavior.

Conclusion

Research has shown that cues in the peripheral visual field help in visual behavior to guide exploration. In our study, we showed that individuals with RP who experience visual-field loss only adapt their viewing behavior according to individual strategies—not on a group level. Image size is a crucial factor affecting individual strategies. Further research focusing on these individual strategies might open novel possibilities to develop new optical devices that help individuals with RP in visual navigation.

Keywords: eye tracking, retinitis pigmentosa, peripheral visual-field loss, overt attention, spatial exploration, visual exploitation

Acknowledgments

We gratefully acknowledge financial support for PK from the European Commission (H2020 FETPROACT-2014, SEP-21014273, socSMCs, ID: 641321). Moreover, we acknowledge support from the Open Access Publishing Fund of Osnabrück University.

RRG, PK, and MBH designed the experiment; RRG, KJ, AH, and AW performed the experiment;

RRH and PK analyzed the data; RRG, PK, and MBH wrote the manuscript.

*PK and MBH share senior authorship.
Commercial relationships: none.
Corresponding author: Ricardo Ramos Gameiro.
Email: rramosga@uni-osnabrueck.de.
Address: Institute of Cognitive Science, University of Osnabrück, Osnabrück, Germany.

References

Açık, A., Sarwary, A., Schultze-Kraft, R., Onat, S., & König, P. (2010). Developmental changes in natural viewing behavior: Bottom-up and top-down differences between children, young adults and older adults. *Frontiers in Psychology*, *1*:207.

Bahill, A. T., Adler, D., & Stark, L. (1975). Most naturally occurring human saccades have magnitudes of 15 degrees or less. *Investigative Ophthalmology & Visual Science*, *14*, 468–469.

Berson, E. L., Sandberg, M. A., Rosner, B., Birch, D. G., & Hanson, A. H. (1985). Natural course of retinitis pigmentosa over a three-year interval. *American Journal of Ophthalmology*, *99*(3), 240–251.

Bindemann, M. (2010). Scene and screen center bias early eye movements in scene viewing. *Vision Research*, *50*(23), 2577–2587.

Boucart, M., Lenoble, Q., Quettelart, J., Szaffarczyk, S., Despretz, P., & Thorpe, S. J. (2016). Finding faces, animals, and vehicles in far peripheral vision. *Journal of Vision*, *16*(2):10, 1–13, https://doi.org/10.1167/16.2.10. [PubMed] [Article]

Boucart, M., Moroni, C., Thibaut, M., Szaffarczyk, S., & Greene, M. (2013). Scene categorization at large visual eccentricities. *Vision Research*, *86*, 35–42.

Broadbent, D. E. (1958). The effects of noise on behaviour. *Perception and communication* (pp. 81–107). Elmsford, NY: Pergamon Press.

Carrasco, M. (2011). Visual attention: The past 25 years. *Vision Research*, *51*(13), 1484–1525.

Cohen, J. D., McClure, S. M., & Yu, A. J. (2007). Should I stay or should I go? How the human brain manages the trade-off between exploitation and exploration. *Philosophical Transactions of the Royal Society B: Biological Sciences*, *362*(1481), 933–942.

Cristino, F., Mathôt, S., Theeuwes, J., & Gilchrist, I. D. (2010). ScanMatch: A novel method for comparing fixation sequences. *Behavior Research Methods*, *42*(3), 692–700.

Desimone, R., & Duncan, J. (1995). Neural mechanisms of selective visual attention. *Annual Review of Neuroscience*, *18*, 193–222.

Deubel, H., & Schneider, W. X. (1996). Saccade target selection and object recognition: Evidence for a common attentional mechanism. *Vision Research*, *36*(12), 1827–1837.

Dewhurst, R., Nyström, M., Jarodzka, H., Foulsham, T., Johansson, R., & Holmqvist, K. (2012). It depends on how you look at it: Scanpath comparison in multiple dimensions with MultiMatch, a vector-based approach. *Behavior Research Methods*, *44*(4), 1079–1100.

Egeth, H. (1967). Selective attention. *Psychological Bulletin*, *67*(1), 41–57.

Fischer, B., & Breitmeyer, B. (1987). Mechanisms of visual attention revealed. *Neuropsychologia*, *25*, 73–83.

Foulsham, T., Walker, E., & Kingstone, A. (2011). The where, what and when of gaze allocation in the lab and the natural environment. *Vision Research*, *51*(17), 1920–1931.

Gajewski, D. A., Pearson, A. M., Mack, M. L., Bartlett, F. N., III, & Henderson, J. M. (2004). Human gaze control in real world search. In L. Paletta, J. K. Tsotsos, E. Rome, & G. Humphreys (Eds.), *Attention and performance in computational vision* (pp. 83–99). Berlin, Heidelberg, Germany: Springer.

Geisler, W. S., & Cormack, L. L. (2011). Models of overt attention. In S. P. Liversedge, I. D. Gilchrist, & S. Everling (Eds.), *The Oxford handbook of eye movements* (pp. 439–454). Oxford, UK: Oxford University Press.

Grover, S. (1998). Patterns of visual field progression in patients with retinitis pigmentosa. *Ophthalmology*, *105*(6), 1069–1075.

Gruber, N., Müri, R. M., Mosimann, U. P., Bieri, R., Aeschimann, A., Zito, G. A., … Nef, T. (2014). Effects of age and eccentricity on visual target detection. Frontiers in Aging Neuroscience, *5*:101.

Hamel, C. (2006). Retinitis pigmentosa. *Orphanet Journal of Rare Diseases*, *1*(1):40.

Hartong, D. T., Berson, E. L., & Dryja, T. P. (2006). Retinitis pigmentosa. *The Lancet*, *368*(9549), 1795–1809.

Hausser, J., & Strimmer, K. (2009). Entropy inference and the James–Stein estimator, with application to nonlinear gene association networks. *Journal of Machine Learning Research*, *10*, 1469–1484.

Henderson, J. M., & Anes, M. D. (1994). Roles of object-file review and type priming in visual

identification within and across eye fixations. *Journal of Experimental Psychology: Human Perception and Performance*, *20*(4), 826–839.

Hoffman, J. E., & Subramaniam, B. (1995). The role of visual attention in saccadic eye movements. *Perception & Psychophysics*, *57*(6), 787–795.

Itti, L., & Koch, C. (2001). Computational modelling of visual attention. *Nature Reviews Neuroscience*, *2*(3), 194–203.

Kaspar, K. (2013). What guides visual overt attention under natural conditions? Past and future research. *ISRN Neuroscience*, *2013*, 868491.

Kaspar, K., Hloucal, T.-M., Kriz, J., Canzler, S., Ramos Gameiro, R., Krapp, V., & König, P. (2013). Emotions' impact on viewing behavior under natural conditions. *PLoS One*, *8*(1), e52737.

Kaspar, K., & König, P. (2012). Emotions and personality traits as high-level factors in visual attention: A review. *Frontiers in Human Neuroscience*, *6*, 321.

Kaspar, K., Ramos Gameiro, R., & König, P. (2015). Feeling good, searching the bad: Positive priming increases attention and memory for negative stimuli on webpages. *Computers in Human Behavior*, *53*, 332–343.

Kietzmann, T. C., Geuter, S., & König, P. (2011). Overt visual attention as a causal factor of perceptual awareness. *PLoS One*, *6*(7), e22614.

Kietzmann, T. C., & König, P. (2015). Effects of contextual information and stimulus ambiguity on overt visual sampling behavior. *Vision Research*, *110*, 76–86.

Kowler, E. (2011). Eye movements: The past 25 years. *Vision Research*, *51*(13), 1457–1483.

Land, M. F. (2009). Vision, eye movements, and natural behavior. *Visual Neuroscience*, *26*(1), 51–62.

Liversedge, S. P., & Findlay, J. M. (2000). Saccadic eye movements and cognition. *Trends in Cognitive Sciences*, *4*(1), 6–14.

Loschky, L. C., Fortenbaugh, F. C., & Levi, D. M. (2017). Scene perception from central to peripheral vision. *Journal of Vision*, *17*(1):6, 1–5, https://doi.org/10.1167/17.1.6. [PubMed] [Article]

Luo, G., Vargas-Martin, F., & Peli, E. (2008). The role of peripheral vision in saccade planning: Learning from people with tunnel vision. *Journal of Vision*, *8*(14):25, 1–8, https://doi.org/10.1167/8.14.25. [PubMed] [Article]

Martinez-Conde, S., Macknik, S. L., & Hubel, D. H. (2004). The role of fixational eye movements in visual perception. *Nature Reviews Neuroscience*, *5*(3), 229–240.

McPhee, L. C., Scialfa, C. T., Dennis, W. M., Ho, G., & Caird, J. K. (2004). Age differences in visual search for traffic signs during a simulated conversation. *Human Factors*, *46*(4), 674–685.

Najemnik, J., & Geisler, W. S. (2005, March 17). Optimal eye movement strategies in visual search. *Nature*, *434*(7031), 387–391.

Parkhurst, D., & Niebur, E. (2003). Scene content selected by active vision. *Spatial Vision*, *16*(2), 125–154.

Parmeggiani, F., Sorrentino, S.F., Ponzin, D., Barbaro, V., Ferrari, S., & Di Iorio, E. (2011). Retinitis pigmentosa: Genes and disease mechanisms. *Current Genomics*, *12*(4), 238–249.

Pelz, J. B., & Canosa, R. (2001). Oculomotor behavior and perceptual strategies in complex tasks. *Vision Research*, *41*(25–26), 3587–3596.

Posner, M. I. (1980). Orienting of attention. *Quarterly Journal of Experimental Psychology*, *32*(1), 3–25.

Rajashekar, U., Bovik, A. C., & Cormack, L. K. (2006). Visual search in noise: Revealing the influence of structural cues by gaze-contingent classification image analysis. *Journal of Vision*, *6*(4):7, 379–386, https://doi.org/10.1167/6.4.7. [PubMed] [Article]

Ramos Gameiro, R., Kaspar, K., König, S. U., Nordholt, S., & König, P. (2017). Exploration and exploitation in natural viewing behavior. *Scientific Reports*, *7*(1):2311.

Razali, N. M., & Wah, Y. B. (2011). Power comparisons of Shapiro–Wilk, Kolmogorov–Smirnov, Lilliefors and Anderson–Darling tests. *Journal of Statistical Modeling and Analytics*, *2*(1), 21–33.

Rosenbach, O. (1903). Ueber monokulare Vorherrschaft beim binokularen Sehen. *Münchener Medizinische Wochenschrift*, *30*, 1290–1292.

Rosenholtz, R. (2016). Capabilities and limitations of peripheral vision. *Annual Review of Vision Science*, *2*(1), 437–457.

Rosenholtz, R., Huang, J., Raj, A., Balas, B. J., & Ilie, L. (2012). A summary statistic representation in peripheral vision explains visual search. *Journal of Vision*, *12*(4):14, 1–17, https://doi.org/10.1167/12.4.14. [PubMed] [Article]

Senedecor, G. W., & Cochran, W. G. (1989). *Statistical methods* (8th ed.). Ames, IA: Iowa State University Press.

Shinoda, H., Hayhoe, M. M., & Shrivastava, A. (2001). What controls attention in natural environments? *Vision Research*, *41*(25–26), 3535–3545.

Staugaard, C. F., Petersen, A., & Vangkilde, S. (2016).

Eccentricity effects in vision and attention. *Neuropsychologia*, *92*, 69–78.

Tatler, B. W. (2007). The central fixation bias in scene viewing: Selecting an optimal viewing position independently of motor biases and image feature distributions. *Journal of Vision*, *7*(14):4, 1–17, https://doi.org/10.1167/7.14.4. [PubMed] [Article]

Tatler, B. W., Baddeley, R. J., & Vincent, B. T. (2006). The long and the short of it: Spatial statistics at fixation vary with saccade amplitude and task. *Vision Research*, *46*(12), 1857–1862.

Unema, P. J. A., Pannasch, S., Joos, M., & Velichkovsky, B. M. (2005). Time course of information processing during scene perception: The relationship between saccade amplitude and fixation duration. *Visual Cognition*, *12*(3), 473–494.

van Diepen, P. M. J., De Graef, P., & D'Ydewalle, G. (1995). Chronometry of foveal information extraction during scene perception. *Studies in Visual Information Processing*, *6*, 349–362.

Wahn, B., & König, P. (2015). Audition and vision share spatial attentional resources, yet attentional load does not disrupt audiovisual integration. *Frontiers in Psychology*, *6*, 1084.

Weber, J., & Klimaschka, T. (1995). Test time and efficiency of the dynamic strategy in glaucoma perimetry. *German Journal of Ophthalmology*, *4*(1), 25–31.

Wilming, N., Betz, T., Kietzmann, T. C., & König, P. (2011). Measures and limits of models of fixation selection. *PLoS One*, *6*(9), e24038.

Wilming, N., Onat, S., Ossandón, J. P., Açik, A., Kietzmann, T. C., Kaspar, K., ... König, P. (2017). An extensive dataset of eye movements during viewing of complex images. *Scientific Data*, *4*: 160126.